Carbon antisite clusters in SiC: A possible pathway to the D_{II} center

Alexander Mattausch,* Michel Bockstedte, and Oleg Pankratov
Lehrstuhl für Theoretische Festkörperphysik, Universität Erlangen-Nürnberg, Staudtstrasse 7, D-91058 Erlangen, Germany
(Received 23 October 2002; revised manuscript received 17 November 2003; published 29 January 2004)

The photoluminescence center D_{II} is a persistent intrinsic defect which is common in all SiC polytypes. Its fingerprints are the characteristic phonon replicas in luminescence spectra. We perform *ab initio* calculations of vibrational spectra for various defect complexes and find that carbon antisite clusters exhibit vibrational modes in the frequency range of the D_{II} spectrum. The clusters possess very high binding energies which guarantee their thermal stability—a known feature of the D_{II} center. The dicarbon antisite $(C_2)_{Si}$ (two carbon atoms sharing a silicon site) is an important building block of these clusters.

DOI: 10.1103/PhysRevB.69.045322 PACS number(s): 63.20.Pw, 61.72.−y, 78.55.−m

I. INTRODUCTION

Many unique features of SiC, such as the wide band gap and the very high electrical and thermal stability, render this semiconductor especially important for high-power, high-frequency, and high-temperature applications. As for any semiconductor material, the identification and understanding of structural defects and impurities is the key to the technological control of SiC. This is especially important in connection with the ion implantation, which is inevitably accompanied by the generation of intrinsic defects. Some of these defects are thermally very stable. Two important examples are the photoluminescence (PL) centers D_I (Ref. 1) and D_{II} (Ref. 2). Although the centers have been extensively studied over the past 30 years,[1–7] their microscopic origin remained unclear. In this work we study carbon antisite clusters and their possible relevance to D_{II}-type centers.

D_{II} centers are always present in ion-implanted and annealed SiC samples, regardless of the implanted species and the polytype. They were also found (in low concentration) in as-grown material.[4] The abundance of D_{II} centers increases significantly at high annealing temperatures (above 1300 °C) and the center is thermally stable up to 1700 °C.[4] These properties imply that the D_{II} centers are intrinsic defect complexes. The D_{II} luminescence originates from the recombination of an exciton bound to the defect. The spectra are usually identified by the main zero-phonon line. The important specific feature of D_{II} are characteristic phonon replicas above the SiC phonon spectrum. In the original experiments in 3C-SiC the strongest five replicas were highlighted.[2] In later experiments[7,6] in 4H and 6H-SiC additional localized vibrational modes (LVM's) were observed [more than 12 LVM's have been counted in 4H-SiC (Ref. 6)]. Many of these observed modes are polytype independent. A comparison of the spectra from Ref. 7 and the earlier Ref. 2 reveals that more than the five highlighted LVM's may also be contained in the 3C spectrum. Their spectral density resembles the phonon density of states in diamond, indicating that a carbon-dominated defect is responsible for the observed spectrum.

In this work we consider a number of carbon-related defects in SiC: the carbon di-interstitial, which was the first suggested model for the D_{II} center,[2] the carbon antisite, the carbon split interstitials, and several carbon clusters. Comparing the calculated LVM's with the experimental D_{II} spectra we are able to unequivocally rule out all candidates except the carbon antisite clusters. The latter are the only defects that provide a rich LVM spectrum similar to that of the D_{II} center. The core structure of all these clusters is the dicarbon antisite $(C_2)_{Si}$ (cf. Fig. 1 left) which acts as an aggregation center for further carbon atoms. In this paper we will first present our results for the dicarbon antisite and then consider the formation of more complex defect clusters. We calculate the LVM's associated with these defects and compare them with the D_{II} spectrum. Although theoretically all these defects can acquire different charge states, we focus on the neutral state as the most relevant for PL. For excitons bound to a charged defect more nonradiative recombination channels are open, and they are unlikely to be seen in PL experiments.[8] We also find that the formation kinetics of the carbon clusters agrees with the known features of the D_{II} center. These results indicate that although neither of the considered defects can alone explain all features of the D_{II} center, the carbon antisite clusters may serve as a core structure of D_{II}-type defects.

II. METHOD

We employ an *ab initio* density-functional theory approach as implemented in the software package FHI96SPIN.[9]

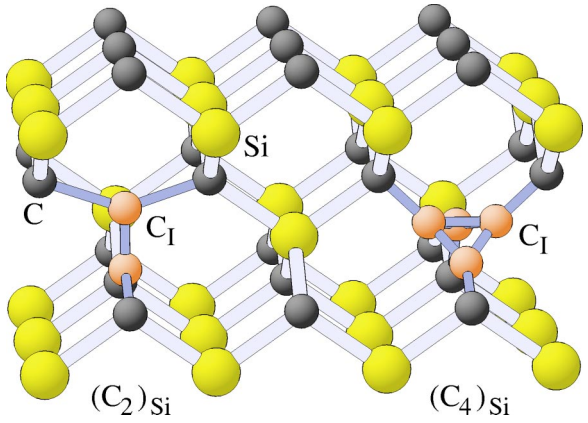

FIG. 1. Structure of the dicarbon antisite $(C_2)_{Si}$ and a carbon cluster with four atoms on a silicon site $(C_4)_{Si}$ in 3C-SiC.

Smooth norm-conserving pseudopotentials of the Troullier-Martin type[10] and a plane-wave basis set with a cutoff energy of 30 Ry are used. The exchange-correlation potential is approximated within the local spin-density approximation (LSDA) in the parametrization of Perdew and Zunger.[11] In order to reduce the artificial defect-defect interaction, large supercells with 216 lattice sites for 3C-SiC and 128 sites for 4H-SiC are used for all calculations of the defect energetics. For the 216-site cell, the Brillouin zone is sampled by the Γ point, whereas for the hexagonal 128-site cell a special Monkhorst and Pack[12] $2\times2\times2$ mesh is used. The values of the formation energies are given assuming silicon-rich conditions. Under carbon-rich conditions they should be reduced by roughly $3\Delta H_f = 1.74$ eV, where $-\Delta H_f$ is the heat of formation of SiC. The vibrational properties are calculated using the *frozen phonon* method. The dynamical matrix

$$\Phi_{ij} = \frac{1}{\sqrt{m_i m_j}} \frac{\partial^2 E}{\partial Q_i Q_j} = \frac{1}{\sqrt{m_i m_j}} \frac{\partial F_i}{\partial Q_j}$$

is calculated by applying displacements Q_j from the equilibrium configuration and evaluating the force derivatives $\partial F_i / \partial Q_j$. To obtain noticeable energy changes, the displacements Q_j ought to be much larger than realistic phonon amplitudes. Therefore it is important to eliminate the anharmonic contribution when evaluating Φ_{ij}. We do this by applying three different values of the displacement and extracting the linear force constant from a polynomial expansion of the forces. The forces have been converged to a relative accuracy of 10^{-4}. For 3C-SiC, the dynamical matrix is evaluated for a supercell with 64 or 216 sites. The experimental bulk phonon modes are reproduced within 5% by this method. Yet the polarization splitting of the transverse-optical (TO) and the longitudinal-optical (LO) modes at the Γ point is missing, since the macroscopic polarization of the crystal is incompatible with the periodic boundary conditions imposed on the supercell. We obtain a triple degenerate mode at 115.3 meV, in place of the TO mode of 98.7 meV and the LO mode of 120 meV.[13] For 4H-SiC and for large clusters in 3C-SiC, the computational cost of evaluating the dynamical matrix of the whole 128-site or 216-site supercell is prohibitively large. In these cases we constrain the LVM calculation to the defect molecule (i.e., the dumbbell and its nearest neighbors) embedded in a supercell. We have examined the error resulting from the defect molecule approximation and from the uncertainty in the lattice constant. The results of these tests for a dicarbon antisite in 3C-SiC (see below) are shown in Fig. 2. The lines represent the frequencies of the LVM's versus the defect molecule size calculated at the theoretical (LSDA) lattice constant. The frequencies shift within the gray area when the lattice constant is increased towards the experimental value of 8.239 bohr. The black bars are the same frequency ranges, but in this case both the electronic structure calculation and the LVM calculation have been performed in a 64-site cell. We have also verified that under the pressure exerted by the periodic array of defects onto the lattice the lattice constant lies between the indicated limits. The LVM's variation due to the uncertainty in the lattice constant is thus less than 10 meV. It is also apparent that the defect molecule approximation affects the least localized modes 1 and (to a much lesser extent) 2. The largest effect on the accuracy has the inclusion of the full supercell, which shifts the mode 1 by 14 meV in the 216-site cell. Compared to the full 64-site cell, the mode 1 is only 2 meV higher.

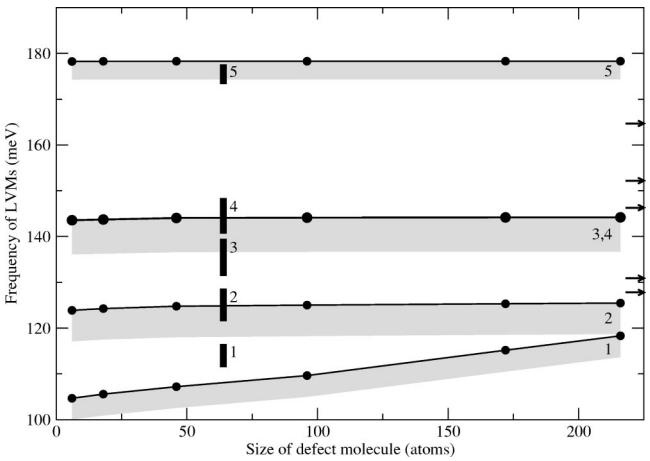

FIG. 2. Defect modes of $(C_2)_{Si}$ vs the defect molecule size in a 216-site cell. The straight line denotes the frequency at the theoretical lattice constant, the gray area is the frequency shift for the variation of the lattice constant between its theoretical and experimental value. The black bars are the corresponding values for the 64-site cell as given in Table I, the arrows indicate the phonon replicas of the D_{II} center (Ref. 2).

III. THE DICARBON ANTISITE

Let us now consider one by one the candidates for the D_{II} center as listed above. First, we find that the originally suggested carbon di-interstitial has a formation energy of about 12 eV. This is extremely high even for SiC and practically rules out this model. A similar defect is the carbon split interstitial $C_{sp\langle100\rangle}$, i.e., a pair of carbon atoms sharing the same (carbon) site and pointing in $\langle100\rangle$ direction (in 3C-SiC). This defect also possesses a short carbon-carbon bond and it is energetically the most favorable carbon interstitial.[14] The second lowest carbon interstitial is the carbon-silicon split interstitial $C_{spSi\langle100\rangle}$ (a carbon and a silicon atom on a silicon site). Here the additional carbon atom is also connected to its nearest neighbors by short carbon-carbon bonds. However, according to our calculations both defects are very mobile,[15] which is in conflict with the thermal stability of the D_{II} center. In addition, we find the LVM's of both defects are not compatible with the D_{II} spectrum. The neutral carbon split interstitial $C_{sp\langle100\rangle}$ in the tilted structure[15] has two LVM's at 120.4 and 188.7 meV and LVM's in the phonon gap. The carbon-silicon split interstitial $C^{2+}_{spSi\langle100\rangle}$ possesses a richer vibrational spectrum but still with only three nondegenerate LVM's above the bulk spectrum. This also does not match the number of the characteristic D_{II} lines. Another possible candidate could be the carbon antisite C_{Si}. Following the carbon vacancy V_C it is the second most abundant defect in SiC. However, it shows only vibrational resonances in the bulk phonon spectrum and has no true LVM's. Also

TABLE I. LVM's of $(C_2)_{Si}$ and $((C_2)_{Si})_2$ in the neutral charge state in meV calculated at the LSDA lattice constant. *ls* denotes the low-spin, *hs* the high-spin state. The subscripts *h* and *k* refer to the hexagonal and the cubic sites. For 4H-SiC and $((C_2)_{Si})_2$ the defect molecule approximation has been used. For the D_{II} center only the five highlighted frequencies are given (cf. Refs. 2 and 7).

LVM	3C				4H					
	$(C_2)_{Si}$, ls	$(C_2)_{Si}$, hs	$((C_2)_{Si})_2$	Expt.	$(C_2)_{Si,h}$, ls	$(C_2)_{Si,h}$, hs	$(C_2)_{Si,k}$, ls	$(C_2)_{Si,k}$, hs	$((C_2)_{Si})_{2,hk}$	Expt.
1	116.4	107.6	123.3	127.8	103.0	100.2	102.3	101.5	119.6	127.1
2	128.5	123.2	125.6	130.9	121.9	121.0	119.7	120.7	132.2	129.8
3	139.4	141.7	127.1	146.3	136.2	136.4	135.0	136.2	147.0	146.1
4	148.3	141.8	139.3	152.2	139.3	137.6	139.1	137.6	160.2	152.4
5	177.5	177.5	168.6	164.7	179.4	177.1	178.0	177.0	162.4	164.4
6			169.7							

small clusters of carbon interstitials do not provide LVM's compatible with the D_{II} spectrum.[16]

The simplest candidate that possesses the main features of the D_{II} center is the dicarbon antisite $(C_2)_{Si}$ that we have already mentioned above in connection with Fig. 2. The dumbbell of two carbon atoms sharing a silicon site (highlighted atoms in Fig. 1 left) is surrounded by a tetrahedron of four carbon atoms. In 3C-SiC the dumbbell is pointing in $\langle 100 \rangle$ direction whereas in 4H-SiC it is oriented either along the $\langle 10\bar{1}1 \rangle$ or the $\langle \bar{1}011 \rangle$ direction. Depending on the Fermi level, the defect may acquire the charge states from 2^+ through 2^-.

We find that the dicarbon antisite has a relatively low formation energy. For the neutral charge state the values are 6.7 eV and 7.8 eV in 3C and 4H polytypes, respectively. In 4H-SiC two possible substitutional configurations exist, i.e., hexagonal (*h*) and cubic (*k*), but the formation energy at these two sites only differs by 0.1 eV. These values are comparable to the formation energies of $C_{sp\langle 100 \rangle}$ and $C_{spSi\langle 100 \rangle}$. Still, the calculated formation energy indicates that its equilibrium abundance is too low for experimental observation. Hence kinetic effects should play an important role in the dicarbon antisite formation. On the other hand, once created, the defect has a very high stability, as reflected by the high binding energy. Before we turn to kinetic aspects, we discuss the electronic properties and the LVM's of the dicarbon antisite.

In 3C-SiC, the dicarbon antisite possesses two degenerate defect orbitals with energy levels in the band gap. In the neutral charge state these orbitals are occupied by two electrons, which can form either a spin-0 (low-spin) or a spin-1 (high-spin) configuration. According to the calculation, the high-spin state is about 80 meV lower in energy than the low-spin state. This energy difference is, however, too small to uniquely determine the ground-state spin configuration. For this reason we consider both options. The defect wave function consists of bonds between the three upper carbon atoms and the three lower carbon atoms of the defect tetrahedron (cf. Fig. 1 left). In the low-spin configuration, one of these bonds is fully occupied, resulting in a splitting of the defect levels and a Jahn-Teller distortion, with the upper or the lower pair of the tetrahedron being stretched. This reduces the original D_{2d} symmetry to C_{2v}. In the high-spin configuration, both bonds are equally occupied, retaining the degeneracy and the D_{2d} symmetry. As we discuss below, this geometrical difference is reflected in the vibrational modes of the defect. In 4H-SiC, the high-spin state is about 120 meV lower than the low-spin state, which is—as in 3C-SiC—a very small energy difference. Due to the lower symmetry of the crystal, the symmetry group is always C_{1h}. The defect's structure on the cubic and the hexagonal site is qualitatively similar.

As outlined above, the dicarbon antisite is the simplest defect that possesses LVM's that are similar to the phonon spectrum of the D_{II} center. The calculated frequencies (using a 64-site supercell) for the neutral charge state in low-spin and high-spin configurations are listed in Table I along with the experimental data for the five characteristic D_{II} phonon modes and our calculated results for the two neighboring dicarbon antisites. We see that in the 3C polytype the low-spin configuration provides a LVM pattern similar to the five phonon replicas of D_{II}. Similar results are obtained for 4H-SiC, except that the frequencies of the modes 1 to 4 are lowered due to the defect molecule approximation.

In spite of a different crystal symmetry, the vibrational patterns of the LVM's in 3C- and 4H-SiC are very similar, owing to the localized nature of the vibrational modes. The highest mode 5 is a stretching vibration, where the two atoms of the dumbbell oscillate against each other. Its calculated frequency is about 8% higher than the experimental value. However, this is the usual accuracy of these defect calculations.[17] The modes 3 and 4 represent an oscillation of one of the dumbbell atoms against its neighbors. In 3C-SiC, these modes are affected by the Jahn-Teller distortion of the low-spin configuration. As expected from the symmetry, the modes are degenerate in the high-spin and nondegenerate in the low-spin case. This effect can also be seen in Fig. 2, where the 216-site calculation, although performed spin unpolarized, has been performed in a high-spin-like configuration. Considering the small energy difference between the high-spin and the low-spin configuration both options should be allowed. In addition to the already mentioned clustering of carbon atoms, this may be a source of further lines in the luminescence spectra. In 4H-SiC, the modes 3 and 4 are always nondegenerate, although the splitting in the high-spin configuration is smaller than in the low-spin configuration, due to the lower symmetry of the crystal field. The mode 2 describes the vibration of the dumbbell along its axis against

the enclosing tetrahedron. The mode 1 is the least localized mode and therefore it is most affected by the employed supercell technique. This mode corresponds to a breathinglike vibration of the enclosing tetrahedron. While for the low-spin case the breathing mode lies above the highest bulk vibration, it is in resonance with the bulk spectrum and lies 8 meV below the calculated value of the highest bulk mode for the high-spin case in a 64-site cell. This is in agreement with Gali *et al.* (Ref. 18) who considered the high-spin state of $(C_2)_{Si}$. In 4H-SiC, a similar behavior is not obvious from our results, as the effect may be masked by the defect molecule approximation. In addition to the high-frequency LVM's discussed above, we also find maxima of the vibrational density of states in the phonon band gap.

It is noteworthy that the results do not change significantly for different possible charge states of the defect.[19,20] We observe a slight lowering of the LVM's frequencies with the increase of the number of localized electrons, resulting from an expansion of the defect molecule due to the occupation of the bonds. For 3C-SiC, the modes 3 and 4 are degenerate in the charge states 2^+ and 2^-, since the electronic defect levels are either empty or fully occupied, and a Jahn-Teller distortion is suppressed.

IV. CLUSTERING OF CARBON ATOMS

Usually, the D_{II} center is observed in ion-implanted and annealed samples. It is stable up to temperatures of 1700 °C. This and the previously discussed low equilibrium concentration suggest a kinetically controlled formation of this defect from nonequilibrium vacancies and interstitials. At first, a carbon antisite is formed via a recombination of a carbon interstitial with a silicon vacancy. It merges then with a mobile carbon split interstitial, producing a dicarbon antisite with a high binding energy that ranges from 3.9 eV ($(C_2)_{Si}^{2+}$) to 5.1 eV ($(C_2)_{Si}^{2-}$). The dicarbon antisite can serve as a condensation center for larger clusters. Such clusters grow by aggregating carbon split interstitials around the core. Adding a further carbon atom to the dicarbon antisite releases a binding energy of 4.8 eV. Binding one more carbon interstitial to this complex yields a very small cluster of four carbon atoms at a silicon site (cf. Fig. 1 right). According to our calculations the energy of 2.8 eV is needed to remove a carbon atom from this structure. However, for this defect we obtain LVM's well above the D_{II} spectrum. A detailed discussion of carbon clusters will be given elsewhere.[16]

In addition to the clusters located around a single silicon site, aggregates of several dicarbon antisites are also possible. A pair of the dicarbon antisites in 3C-SiC $((C_2)_{Si})_2$ is shown in Fig. 3. In 4H-SiC three different configurations, which can be compared to its 3C-SiC counterpart, are possible when the two diantisites occupy two cubic (*kk*), two hexagonal (*hh*) or cubic-hexagonal (*kh*) sites. As an exemplary structure we have considered in detail the *kh* configuration, which has a local geometry similar to the 3C-SiC case (Fig. 3), but the bond length between the neighboring dicarbon antisites is shorter. We found that this defect is very stable in both polytypes: in 3C-SiC it costs about 5.9 eV to remove a carbon atom, whereas in 4H-SiC this energy is 6.7

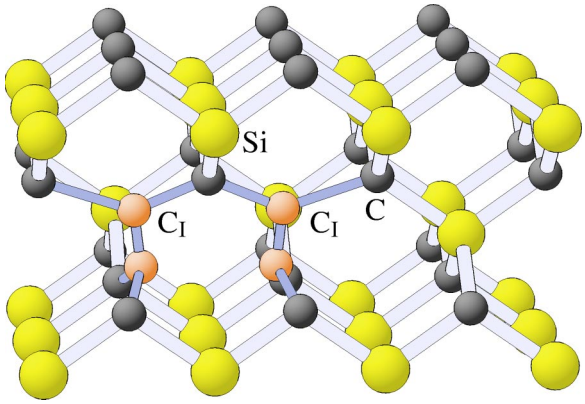

FIG. 3. Structure of a pair of dicarbon antisites $((C_2)_{Si})_2$ in 3C-SiC.

eV. The calculated LVM's of both complexes are given in Table I. They have been calculated using the defect molecule approximation that allows the vibration of the two dumbbells and of the surrounding carbon neighbors within the 216- (3C-SiC) and 128- (4H-SiC) site cell. As discussed above, the numerical results are affected by the defect molecule approximation. Alternatively, one could work with the smaller 64-site cell which would allow to calculate the dynamical matrix of the whole cell. However, we find that in this cell the electronic structure is so strongly distorted by the proximity effects that it is unacceptable for the analysis of the LVM's. For the pair of dicarbon antisites the highest almost degenerate modes 5 and 6 involve a stretching vibration of the dumbbells, similar to the lone dicarbon antisite. Due to the interaction of the dumbbells these modes become softer and combine into antisymmetric and symmetric vibrations. The modes 3 and 4 represent a motion of the two lower and upper carbon atoms of the dumbbells in bond direction against their surrounding neighbors, respectively. In 4H-SiC, the defect shows a similar behavior, but the energy of all modes is by about 8 meV lower than in 3C-SiC so that the lowest mode (with an energy of 114.4 meV) drops into the bulk phonon spectrum. This effect and also the larger frequency difference between the stretching modes reflects the stronger relaxation of the defect in this polytype. We have recently learned that Gali *et al.* calculated the LVM's of the *kk* configuration, finding results similar to the 3C-SiC values, and speculated that this defect was the D_{II} center.[21] As the *kk* configuration has a 3C-like environment (in contrast to the *kh* configuration), the similarity to 3C-SiC is quite natural. However, the conjecture that the $((C_2)_{Si})_2$ model completely describes the D_{II} center does not seem to be supported by experimental data. Recent experiments have investigated the multitude of zero-phonon lines[5] (ZPL's) as well as the phonon replicas[6] of the D_{II} center. In 6H-SiC, Sridhara *et al.*[5] concluded from temperature and stress-dependence experiments that the four ZPL's of D_{II} stem from the different excitonic states of the bound exciton (one ground state and three excited states), but not from different binding centers of the same exciton. Regarding the phonon replicas in 4H-SiC more than 12 LVM's and a single ZPL have been

reported by Carlsson *et al.*,[6] which is consistent with the earlier results for 4H and 6H-SiC of Sridhara *et al.*[7] In addition, as we noted above, a comparison of the spectra in 3C,[2] 4H, and 6H-SiC (Ref. 7) indicates that more than five LVM's may be present also in 3C-SiC. The apparent large number of phonon replicas in 4H and 6H-SiC makes it tempting to assume that they originate from different geometrical configurations of the same simple defect. For example, for the $((C_2)_{Si})_2$ in 4H-SiC this would be *kk*, *hh*, and *kh*. This assumption has, however, the following implications. First, it follows that a larger number of LVM's should be present in 6H-SiC than in 4H or 3C-SiC, since less or no inequivalent sites are available in the two latter polytypes. Second, the different configurations should give rise to a multitude of exciton ground-state ZPL's. According to the conclusion of Sridhara *et al.*[5] and the rich vibrational structure contained in all polytypes (cf. discussion above) this is not evident from the experiments. This applies, in particular, to the $((C_2)_{Si})_2$ defect. Furthermore, the LVM pattern of this defect is, in fact, not compatible with the D_{II} spectrum. The small splitting of the two highest LVM's (see Table I), which persists through different polytypes and configurational models, is not observed in the D_{II} spectrum which has nearly equidistant lines. Thus the $((C_2)_{Si})_2$ model alone cannot explain all features of the D_{II} center. Larger carbon clusters are likely to be involved. For such clusters the differences between the polytypes lose their importance. This may be responsible for the polytype-independent LVM's of the D_{II} centers. Further experimental data are necessary to clarify the situation, especially for the 3C polytype, which lacks inequivalent lattice sites.

V. CONCLUSION

In conclusion, we have analyzed the structural, electronic, and vibrational properties of the dicarbon antisite complex. The defect possesses a characteristic vibrational pattern in the frequency range of the D_{II} spectrum, but cannot explain all the phonon replicas observed. Yet, we find that the dicarbon antisite can act as an aggregation center for carbon clusters that allow for a much richer phonon spectrum. All the defect complexes presented above possess very high dissociation energies, which guarantee their high thermal stability. Due to the high formation energies, these defects can exist in as-grown material only in very low concentrations but can be kinetically created during the annealing. Yet, none of the considered defect complexes can explain all features of the D_{II} center. Most probably the D_{II}-type centers are related to larger carbon clusters with the dicarbon antisite playing the role of an elementary building block of the aggregates.

ACKNOWLEDGMENTS

We acknowledge fruitful discussions with W.J. Choyke. This work was supported by the Deutsche Forschungsgemeinschaft within the SiC Research Group.

*Electronic address: Mattausch@physik.uni-erlangen.de

[1] L. Patrick and W.J. Choyke, Phys. Rev. B **5**, 3253 (1972).
[2] L. Patrick and W.J. Choyke, J. Phys. Chem. Solids **34**, 565 (1973).
[3] T. Egilsson, J.P. Bergman, I.G. Ivanov, A. Henry, and E. Janzén, Phys. Rev. B **59**, 1956 (1999).
[4] J.A. Freitas, S.G. Bishop, J.A. Edmond, J. Ryu, and R.F. Davis, J. Appl. Phys. **61**, 2011 (1987).
[5] S.G. Sridhara, F.H.C. Carlsson, J.P. Bergman, A. Henry, and E. Janzén, Mater. Sci. Forum **353-356**, 377 (2001).
[6] F.H.C. Carlsson, S.G. Sridhara, A. Hallén, J.P. Bergman, and E. Janzén, Mater. Sci. Forum **433-436**, 345 (2003).
[7] S.G. Sridhara, D.G. Nizhner, R.P. Devaty, W.J. Choyke, T. Dalibor, G. Pensl, and T. Kimoto, Mater. Sci. Forum **264-268**, 493 (1998); W. J. Choyke (private communication).
[8] A. M. Stoneham, *Theory of Defects in Solids* (Oxford University Press, London, 1975).
[9] M. Bockstedte, A. Kley, J. Neugebauer, and M. Scheffler, Comput. Phys. Commun. **107**, 187 (1997).
[10] M. Fuchs and M. Scheffler, Comput. Phys. Commun. **119**, 67 (1999).
[11] J.P. Perdew and A. Zunger, Phys. Rev. B **23**, 5048 (1981).
[12] H.J. Monkhorst and J.D. Pack, Phys. Rev. B **13**, 5188 (1976).
[13] F. Widulle, T. Ruf, O. Buresch, A. Debernardi, and M. Cardona, Phys. Rev. Lett. **82**, 3089 (1999).
[14] A. Mattausch, M. Bockstedte, and O. Pankratov, Mater. Sci. Forum **353-356**, 323 (2001).
[15] M. Bockstedte, A. Mattausch, and O. Pankratov, Phys. Rev. B **68**, 205201 (2003).
[16] A. Mattausch, M. Bockstedte, and O. Pankratov (unpublished).
[17] R.B. Capaz, A. Dal Pino, and J.D. Joannopoulos, Phys. Rev. B **58**, 9845 (1998).
[18] A. Gali, P. Deák, N.T. Son, and E. Janzén, Mater. Sci. Forum **389-393**, 477 (2002).
[19] A. Mattausch, M. Bockstedte, and O. Pankratov, Physica B **308-310**, 656 (2001).
[20] A. Mattausch, M. Bockstedte, and O. Pankratov, Mater. Sci. Forum **389-393**, 481 (2002).
[21] A. Gali, P. Deák, P. Ordejón, N.T. Son, E. Janzén, and W.J. Choyke, Phys. Rev. B **68**, 125201 (2003).